Generalized Drude model: unification of ballistic and diffusive electron transport

2001 J. Phys.: Condens. Matter 13 3347

(http://iopscience.iop.org/0953-8984/13/14/309)

INSTITUTE OF PHYSICS PUBLISHING JOURNAL OF PHYSICS: CONDENSED MATTER

J. Phys.: Condens. Matter **13** (2001) 3347–3363 www.iop.org/Journals/cm PII: S0953-8984(01)14089-0

Generalized Drude model: unification of ballistic and diffusive electron transport

R Lipperheide, T Weis and U Wille

Abteilung Theoretische Physik, Hahn-Meitner-Institut Berlin, Glienicker Str. 100, D-14109 Berlin, Germany

Received 4 January 2001, in final form 7 February 2001

Abstract

For electron transport in parallel-plane semiconducting structures, a model is developed that unifies ballistic and diffusive transport and thus generalizes the Drude model. The unified model is valid for arbitrary magnitude of the mean free path and arbitrary shape of the conduction band edge profile. Universal formulas are obtained for the current-voltage characteristic in the nondegenerate case and for the zero-bias conductance in the degenerate case, which describe in a transparent manner the interplay of ballistic and diffusive transport. The semiclassical approach is adopted, but quantum corrections allowing for tunnelling are included. Examples are considered, in particular the case of chains of grains in polycrystalline or microcrystalline semiconductors with grain size comparable to, or smaller than, the mean free path. Substantial deviations of the results of the unified model from those of the ballistic thermionic-emission model and of the drift-diffusion model are found. The formulation of the model is one-dimensional, but it is argued that its results should not differ substantially from those of a fully three-dimensional treatment.

1. Introduction

Electron transport in semiconducting structures is *ballistic* if the mean free path is much larger than the characteristic dimensions of the sample, and it is *diffusive* if the mean free path is much smaller than these. In the first case, there is no impurity or lattice scattering, and the current is determined by the ballistic motion in the electric field [1, 2]; in the second case, scattering predominates and is described within the drift-diffusion scheme [3, 4]. In many cases of physical relevance, however, the mean free path is neither large nor small compared with the characteristic dimensions of the sample. Thus, formulas for the current-voltage characteristic have appeared in the literature which combine features of the two limiting types of transport mechanism for particular conduction band edge profiles, e.g. for a single barrier [5–11].

In the present paper, we consider electron transport in parallel-plane semiconducting structures, i.e. structures whose parameters vary in one direction only. We develop a one-dimensional transport model which is valid for any magnitude of the mean free

0953-8984/01/143347+17$30.00

path and any form of the band edge profile, and thus unifies the ballistic and diffusive transport mechanisms. It is based on the idea that the electrons move ballistically in the electric field over intervals with average length equal to a universal mean free path, after which they are thermalized into a state of local equilibrium characterized by a quasi-Fermi level (electrochemical potential). The length of the sample is made up of random configurations of such ballistic intervals. Averaging over these configurations results in a unified description of electron transport, in which purely ballistic and purely diffusive transport appear as limiting cases. We work within the semiclassical approach [12], which allows a concise and transparent formulation. However, quantum tunnelling ('thermionic field emission' [13, 14]) is taken into account in WKB approximation.

The description of transport in terms of ballistic motion over intervals of the average length of the mean free path with thermalization at the end is, of course, also the basis of the Drude model [12,15,16] and of the relaxation-time approximation of the Boltzmann equation. There, however, the further development makes use of the assumption that the mean free path is small compared to the characteristic dimensions of the sample, leading to a diffusive description of the transport. In contrast to this, such an assumption is *not* made in the present work, and the magnitude of the mean free path relative to the sample dimensions determines the relative importance of the ballistic and diffusive transport mechanisms. The unified description thus is a generalization of the Drude model; it is particularly relevant to polycrystalline and microcrystalline materials (in the following indiscriminately referred to as 'polycrystalline materials') when the grain size is comparable to, or smaller than, the mean free path. In this case, the grains must not be considered separately and the sample must be treated as a whole.

Our approach is the semi-phenomenological one commonly used in the description of transport in semiconductor devices (cf. [2]). Its prominent and useful feature is that its results are obtained in closed form, which allows one to analyse the physics of the transport process in a transparent way. We have been able to formulate our model in one dimension. For transport across parallel-plane structures as considered in the present work, a fully three-dimensional treatment of the thermalization process is expected not to change the resulting formulas in a substantial way (cf. section 3.4 below for a more detailed discussion of this point).

In the following section, we introduce the basic assumptions of the unified model and explain the procedure of averaging over the random configurations of ballistic intervals across which the electrons travel without scattering. In section 3, we present our principal result: a universal formula for the current-voltage characteristic reflecting the interplay of ballistic and diffusive transport. This formula generalizes previous expressions proposed for a single barrier. Its distinctive new feature is the appearance of a shape term that depends on the detailed structure of the band edge profile and also explicitly on the mean free path. This term is essential, e.g. for the description of transport in polycrystalline materials. Section 4 deals with two numerical examples. First, we investigate chains of identical grains in polycrystalline materials. Here, the effect of the relative magnitudes of mean free path and characteristic length of the sample, i.e. the relative importance of the ballistic and diffusive mechanisms, is demonstrated explicitly. It is found that the (zero-bias) conductivity, defined as conductance times sample length, generally depends upon the number of grains in the sample. Second, as an example of a degenerate system, we discuss the grain barrier conductance of a highly-doped polycrystalline material as a function of temperature. Section 5 contains a summary and some concluding remarks.

2. The model

2.1. Basic formulation

The unified model is based on the following one-dimensional scheme (cf. figure 1). The length of the sample (extending from $x = 0$ to $x = S$) is covered by a chain of N intervals $\{i\}$ with end points x_{i-1}^N and x_i^N, $i = 1, \ldots, N$ ($x_i^N > x_{i-1}^N$; $x_0^N = 0$, $x_N^N = S$) across which the electrons move ballistically in the field of the conduction band edge potential $E_c(x)$. There may be any number of intervals in a chain, $N = 1, \ldots, \infty$. At the end points of these 'ballistic intervals' (in particular, at the fixed end points of the sample), the electrons are equilibrated (thermalized). These points of local equilibrium are theoretical constructs which may be thought to be connected via thin ideal leads (flat potentials) to large ideal reservoirs in equilibrium, with chemical potentials equal to the quasi-Fermi level at the points [17]. The current flow in a ballistic interval is assumed to result from the injection of electrons at the end points and their transmission through the interval, in line with Landauer's view of conduction as a transmission phenomenon [18–21].

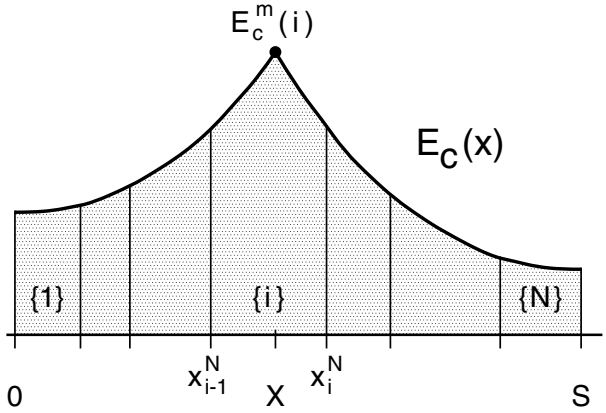

Figure 1. Averaging over the ballistic configurations: single peak of the band edge profile $E_c(x)$ at $x = X$.

The current in the ballistic interval $\{i\}$ is given by

$$j(i) = -e \int_0^\infty \mathrm{d}\epsilon \left[T_i^{\mathrm{L}}(\epsilon + E_c(x_{i-1}))\, f\left(x_{i-1}^N; \epsilon\right) - T_i^{\mathrm{R}}(\epsilon + E_c(x_i))\, f\left(x_i^N; \epsilon\right) \right] \qquad i = 1, \ldots, N \tag{1}$$

where $f(x; \epsilon)$ is the phase space density of the electrons at position x with kinetic energy ϵ of the motion in the x-direction, and $T_i^{\mathrm{L}}(E)$ is the (classical or quantal) probability for ballistic transmission at total energy E from x_{i-1}^N to x_i^N [reversely for $T_i^{\mathrm{R}}(E)$]. Owing to time reversal invariance we have $T_i^{\mathrm{L}}(E) = T_i^{\mathrm{R}}(E)$ [$= T_i(E)$]. For Boltzmann statistics (nondegenerate regime), we have $f(x; \epsilon) = (4\pi m^*/\beta h^3) \exp\{-\beta[\epsilon + E_c(x) - E_F(x)]\}$, and obtain from equation (1)

$$j(i) = -e v_e N_c \mathcal{T}(i) \left[\mathrm{e}^{\beta E_F(x_{i-1}^N)} - \mathrm{e}^{\beta E_F(x_i^N)} \right] \qquad i = 1, \ldots, N. \tag{2}$$

Here, $v_e = (2\pi m^* \beta)^{-1/2}$ is the emission velocity, the factor $N_c = 2(2\pi m^*/\beta h^2)^{3/2}$ is the effective density of states at the conduction band edge, $E_F(x)$ is the quasi-Fermi level at

position x, and $\beta = 1/k_B T$. The factor $\mathcal{T}(i)$ is the thermally averaged probability for ballistic transmission across the interval $\{i\}$,

$$\mathcal{T}(i) = \beta \int_{E_c^{(i)}}^{\infty} \mathrm{d}E \mathrm{e}^{-\beta E}\, T_i(E) \tag{3}$$

where $E_c^{(i)} = \max\{E_c(x_{i-1}), E_c(x_i)\}$ (cf. [22] and [23], section 2.1).

In the classical description, we have $T_i(E) = \Theta(E - E_c^m(i))$, where $E_c^m(i)$ is the maximum of the conduction band edge profile $E_c(x)$ between or at the points x_{i-1}^N and x_i^N. Therefore, equation (2) becomes

$$j(i) = -ev_e N_c \,\mathrm{e}^{-\beta E_c^m(i)} \left[\mathrm{e}^{\beta E_F(x_{i-1}^N)} - \mathrm{e}^{\beta E_F(x_i^N)}\right] \qquad i = 1, ..., N. \tag{4}$$

In what follows, we adhere to the classical description since it allows the greatest transparency, in particular as far as the averaging over ballistic intervals is concerned. The full formulation including tunnelling effects will be presented in section 3.2.

In the stationary case, the current is independent of position, $j(i) = j = \text{const.}$, and we can write equation (4) in the form

$$\mathrm{e}^{\beta E_F(x_i^N)} = \mathrm{e}^{\beta E_F(x_{i-1}^N)} + \frac{j}{ev_e N_c}\,\mathrm{e}^{\beta E_c^m(i)} \qquad i = 1, ..., N. \tag{5}$$

Iterating this relation, we find for a configuration with N ballistic intervals

$$\mathrm{e}^{\beta E_F(S)} - \mathrm{e}^{\beta E_F(0)} = \frac{j}{ev_e N_c} \sum_{i=1}^{N} \mathrm{e}^{\beta E_c^m(i)}. \tag{6}$$

The sum on the right-hand side must be averaged over all possible configurations of the ballistic intervals, i.e. over all positions of their end points x_i^N $(i = 1, \ldots, N-1)$ in the chain of N intervals, where $N = 1, \ldots, \infty$. Introducing the absolute maximum E_c^m of the band edge profile $E_c(x)$ in the interval $[0, S]$, we denote the product of $\exp(-\beta E_c^m)$ with the average of the sum by Ξ,

$$\Xi = \left\langle \sum_{i=1}^{N} \mathrm{e}^{-\beta[E_c^m - E_c^m(i)]} \right\rangle_{\{N, x_i^N\}}. \tag{7}$$

Setting $E_F(0) - E_F(S) = eV$, we then have

$$1 - \mathrm{e}^{-\beta eV} = -\frac{j}{ev_e N_c}\,\mathrm{e}^{\beta E_p}\,\Xi \tag{8}$$

where $E_p = E_c^m - E_F(0)$ is the overall barrier height. The end points of the sample are connected to large ideal reservoirs in equilibrium characterized by the Fermi levels $E_F(0)$ and $E_F(S)$ whose difference determines the voltage bias V [20].

2.2. Averaging over the ballistic configurations

2.2.1. The distribution of the ballistic intervals The distribution of a set of N ballistic intervals, i.e. of the points of equilibrium x_i^N, across the sample of length S is determined in the following way. The probability of an electron to make a collision in the interval $d\xi$ after having traversed a distance ξ since its last collision is given by $\exp(-\xi/l)(d\xi/l)$, where l is the mean free path [12, 16]. Assuming (as in the Drude model) that an electron which collides with an impurity is taken out of the ballistic current and can be counted as equilibrized, we

write the complete distribution of the ballistic intervals in the form of an infinite-dimensional *diagonal matrix* with elements labelled by the number N of ballistic intervals, $N = 1, 2, \ldots$:

$$d\boldsymbol{P} = \left\{ \mathrm{e}^{-S/l}, \ldots, \left[\prod_{i=1}^{N-1} \frac{\mathrm{d}x_i^N}{l}\, \mathrm{e}^{-(x_i^N - x_{i-1}^N)/l}\, \theta\left(x_i^N - x_{i-1}^N\right) \right] \mathrm{e}^{-(S - x_{N-1}^N)/l}, \ldots \right\} = \{\ldots, dP_N, \ldots\}. \tag{9}$$

Here the exponents in the general term cancel out except for the term $(-S/l)$, and we have (recalling $x_0^N = 0$)

$$dP_1 = \mathrm{e}^{-S/l} \qquad dP_N = \mathrm{e}^{-S/l} \prod_{i=1}^{N-1} \frac{\mathrm{d}x_i^N}{l}\, \theta\left(x_i^N - x_{i-1}^N\right) \quad \text{for} \quad N \geqslant 2. \tag{10}$$

This distribution is normalized to unity, since

$$\mathrm{Tr} \int \mathrm{d}\boldsymbol{P} = \left(1 + \sum_{N=2}^{\infty} \int_0^S \frac{\mathrm{d}x_1^N}{l} \int_{x_1^N}^S \frac{\mathrm{d}x_2^N}{l} \cdots \int_{x_{N-2}^N}^S \frac{\mathrm{d}x_{N-1}^N}{l} \right) \mathrm{e}^{-S/l} = 1. \tag{11}$$

Here, the infinite sum over N contains power terms which add up to the exponential $\exp(S/l)$; the evaluation of all quantities considered in the following runs along similar lines.

The average sum (7) can be written as an expectation value of the form

$$\Xi = \left\langle \sum_{i=1}^{N} \mathrm{e}^{-\beta[E_\mathrm{c}^\mathrm{m} - E_\mathrm{c}^\mathrm{m}(i)]} \right\rangle_{\{N, x_i^N\}} = \mathrm{Tr} \int \mathrm{d}\boldsymbol{P}\, \Sigma \tag{12}$$

where we have introduced the infinite-dimensional diagonal matrix

$$\Sigma = \left\{ \ldots, \sum_{i=1}^{N} \mathrm{e}^{-\beta[E_\mathrm{c}^\mathrm{m} - E_\mathrm{c}^\mathrm{m}(i)]}, \ldots \right\} \qquad N = 1, 2, \ldots. \tag{13}$$

2.2.2. The average for a peak in $E_\mathrm{c}(x)$ The case where the conduction band edge profile $E_\mathrm{c}(x)$ has a single peak at the position X somewhere along the sample is illustrated in figure 1. If a ballistic interval $\{i\}$ contains X, we have $E_\mathrm{c}^\mathrm{m}(i) = E_\mathrm{c}(X)$; if it lies to the left (right) of X, we have $E_\mathrm{c}^\mathrm{m}(i) = E_\mathrm{c}(x_i^N)$ $[= E_\mathrm{c}(x_{i-1}^N)]$. Thus we obtain for the average sum

$$\begin{aligned} \Xi = \sum_{N=1}^{\infty} \int \mathrm{d}P_N \sum_{i=1}^{N} \mathrm{e}^{-\beta E_\mathrm{c}^\mathrm{m}} \Big[& \mathrm{e}^{\beta E_\mathrm{c}(x_i^N)}\, \theta\left(X - x_i^N\right) + \mathrm{e}^{\beta E_\mathrm{c}(X)}\, \theta\left(x_i^N - X\right)\, \theta\left(X - x_{i-1}^N\right) \\ & + \mathrm{e}^{\beta E_\mathrm{c}(x_{i-1}^N)}\, \theta\left(x_{i-1}^N - X\right) \Big] \\ = {} & 1 + \widetilde{S}/l \end{aligned} \tag{14}$$

where $E_\mathrm{c}^\mathrm{m} = E_\mathrm{c}(X)$ in the 'reduced sample length'

$$\widetilde{S} = \int_0^S \mathrm{d}x\, \mathrm{e}^{-\beta[E_\mathrm{c}^\mathrm{m} - E_\mathrm{c}(x)]} \tag{15}$$

satisfying $\widetilde{S} \leqslant S$. Special cases are $X = 0$ and $X = S$, when the profile is monotonic.

It is seen that the average sum Ξ for a profile containing a single maximum at a position X inside or at the end of the sample, is given by unity plus the ratio of reduced sample length and mean free path. By the definition of the average sum Ξ, the unit term represents the contribution of the ballistic transmission across the *highest* peak E_c^m of the profile $E_\mathrm{c}(x)$.

2.2.3. The average for a valley in $E_c(x)$ We consider a conduction band edge profile of the type shown in figure 2. It contains two peaks at X_0 and X_1, respectively (without loss of generality, the left peak is assumed to be the higher one), and in between a valley with minimum at Y_1. The average sum over the ballistic intervals *enclosed* by the peaks ($X_0 \leqslant x_{i-1}^N; x_i^N \leqslant X_1$) is given by

$$\Xi = \sum_{N=1}^{\infty} \int \mathrm{d}P_N \sum_{i=1}^{N} \mathrm{e}^{-\beta E_c^m} \left\{ \mathrm{e}^{\beta E_c(x_{i-1}^N)}\, \theta\left(Y_1 - x_i^N\right) + \mathrm{e}^{\beta E_c(x_i^N)}\, \theta\left(x_{i-1}^N - Y_1\right) \right.$$
$$\left. + \left[\mathrm{e}^{\beta E_c(x_{i-1}^N)}\, \theta\left(x_{i-1}^{N*} - x_i^N\right) + \mathrm{e}^{\beta E_c(x_i^N)}\, \theta\left(x_{i-1}^N - x_i^{N*}\right) \right] \theta\left(x_i^N - Y_1\right)\, \theta\left(Y_1 - x_{i-1}^N\right) \right\} \tag{16}$$

where x^* is that position to the right (left) of Y_1 where the profile has the same height as at the point x to the left (right) of Y_1. The average sum over the ballistic intervals contributed by the *left-hand* peak at X_0 is given by equation (14) with $X = X_0$ and the last term in the brackets omitted, and analogously for the *right-hand* peak at X_1. The average sum for the profile of figure 2 can then be evaluated as

$$\Xi = 1 + \widetilde{S}/l + \int_{X_1^*}^{X_1} \frac{\mathrm{d}x}{l} \mathrm{e}^{-|x-x^*|/l} \mathrm{e}^{-\beta E_c(X_0)} \left[\mathrm{e}^{\beta E_c(X_1)} - \mathrm{e}^{\beta E_c(x)} \right] \tag{17}$$

where now $E_c^m = E_c(X_0)$ in $\widetilde{S}$.

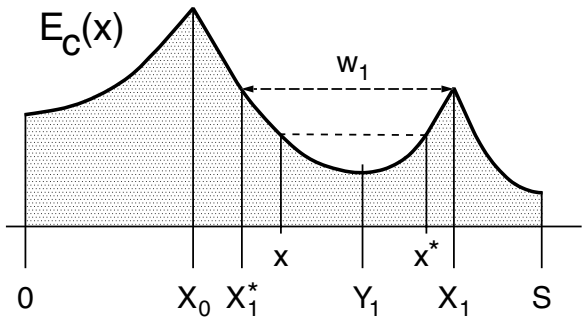

Figure 2. Averaging over the ballistic configurations: single valley of the band edge profile $E_c(x)$. For explanation, see text.

It is seen from formula (17) that for $b_{0,1} \ll l \ll w_1$, where $w_1 = X_1 - X_1^*$ is the width of the valley and $b_{0,1}$ are the 'widths' of the two barriers at $X_{0,1}$, the integral over the second exponential in the brackets can be neglected. Since

$$\int_{X_1^*}^{X_1} \mathrm{d}x\, \mathrm{e}^{-|x-x^*|/l} = l\left(1 - \mathrm{e}^{-w_1/l}\right) \approx l \tag{18}$$

we obtain

$$\Xi = 1 + \widetilde{S}/l + \mathrm{e}^{-\beta[E_c(X_0) - E_c(X_1)]} \tag{19}$$

i.e. we have independent contributions from each peak (first and third terms).

On the other hand, for $S \ll l$ (ballistic regime), the whole integral term in equation (17) can be neglected (together with the term $\widetilde{S}/l$) since it is smaller than $(w_1/l)\exp\{-\beta[E_c(X_0) - E_c(X_1)]\}$. Then Ξ reduces to the unit term, which represents the contribution of the transmission across the higher peak at X_0: this peak 'eclipses' the lower peak at X_1.

3. Current-voltage characteristic

3.1. Classical current-voltage characteristic

In the foregoing, we have considered single peaks and valleys. If the profile contains not just one, but an arbitrary combination of such structures as in a chain of grains in polycrystalline materials, the average sum Ξ for a general band edge profile is given by

$$\Xi = 1 + (\widetilde{S} + \widetilde{\Lambda})/l \tag{20}$$

where we have introduced the 'shape term' $\widetilde{\Lambda}$ for M valleys,

$$\widetilde{\Lambda} = \sum_{v=1}^{M} \int_{X_v^*}^{X_v} \mathrm{d}x \mathrm{e}^{-|x-x^*|/l} \mathrm{e}^{-\beta E_\mathrm{c}^\mathrm{m}} \left[\mathrm{e}^{\beta E_\mathrm{c}(X_v)} - \mathrm{e}^{\beta E_\mathrm{c}(x)}\right]. \tag{21}$$

The contribution of valley v (with adjoining lower maximum X_v) consists of an integral which extends over the width of the valley from X_v^* to X_v. We now define the effective transport length $L = \Xi\, l$, so that

$$L = l + \widetilde{S} + \widetilde{\Lambda}. \tag{22}$$

In compliance with equation (18), we find $\widetilde{\Lambda} < S$.

From equations (8), (20) and (22), we obtain the classical current-voltage characteristic for nondegenerate systems as

$$j = -ev_\mathrm{e} N_\mathrm{c} \mathrm{e}^{-\beta E_\mathrm{p}} \frac{l}{L} (1 - \mathrm{e}^{-\beta eV}). \tag{23}$$

This formula is the principal result of the present work. It is given here in the context of classical transport, where its interpretation is most perspicuous; corrections due to tunnelling will be introduced below.

The properties of the current-voltage characteristic (23) are determined by the barrier height E_p and the ratio l/L. In equation (22) for the effective transport length L, the mean free path l represents the ballistic contribution to the current (this term is associated with the highest peak of the band edge profile). The remaining terms give a quantitative measure of the influence of that part of the electron motion which is not purely ballistic. Their contribution amounts to at most twice the length S of the sample. The reduced sample length $\widetilde{S}$ given by equation (15) represents a contribution that characterizes the band edge profile $E_\mathrm{c}(x)$ in an integral way; it does not manifestly depend on l, only indirectly via the profile (cf. below). The shape term $\widetilde{\Lambda}$ given by equation (21), on the other hand, depends on the detailed structure of the profile as well as explicitly on the mean free path and thus represents the interplay of ballistic and diffusive transport. This term is a distinctive feature of formula (23).

We emphasize that the integrals appearing in the effective transport length L, and in particular the reduced sample length $\widetilde{S}$, result from averaging over ballistic configurations, *not* because l were so small that the sum over intervals could be replaced with an integral, as assumed in the diffusive regime.

The barrier height E_p and the effective transport length L are determined by the band edge profile $E_\mathrm{c}(x)$ which is a solution of the Poisson equation

$$E_\mathrm{c}''(x) = \frac{e}{\epsilon_\mathrm{s}}[-en(x) + Q(x)] \tag{24}$$

where

$$n(x) = N_\mathrm{c} \mathrm{e}^{-\beta[E_\mathrm{c}(x) - E_\mathrm{F}(x)]} \tag{25}$$

is the conduction electron density and $Q(x)$ is the density of fixed charges. In the 'trapping model' for grain boundaries in polycrystalline materials [24–27], which our calculations in section 4 are based upon, the density $Q(x)$ is given by

$$Q(x) = eN_{\mathrm{don}} + \sum_{v=1}^{M} q_v^{\mathrm{t}}\, \delta(x - X_v) \tag{26}$$

where N_{don} is the density of donor atoms (assumed completely ionized), and q_v^{t} is the area density of the charge associated with occupied acceptor-like 'trapping states' localized at the grain boundary at X_v. The donor density N_{don} not only affects the band edge profile $E_{\mathrm{c}}(x)$, but also determines the magnitude of the mean free path l (a simple relation between l and N_{don} is obtained from the analytical expression for the N_{don}-dependence of the electron mobility μ given in [28], using $\mu = ev_{\mathrm{e}}\beta l$). Thus, there is, in general, an indirect relation between $E_{\mathrm{c}}(x)$ and l, which implies an indirect (and generally rather strong) l-dependence of the barrier height E_{p} as well as of the reduced sample length $\widetilde{S}$ and the shape term $\widetilde{\Lambda}$ [as noted above, the latter term also depends explicitly on l, namely via the weight function $\exp(-|x - x^*|/l)$].

When the bias vanishes, the electron density $n(x)$ has the equilibrium form given by expression (25) with $E_{\mathrm{F}}(x) = \text{const.} = E_{\mathrm{F}}(0)$, and we obtain a nonlinear differential equation for $E_{\mathrm{c}}(x)$. In the presence of bias, the Poisson equation (24) must be solved in conjunction with an equation for the current j. In the diffusive limit, this equation is given by the familiar drift-diffusion expression for the current,

$$j = \mu n(x)\frac{\mathrm{d}}{\mathrm{d}x}E_{\mathrm{F}}(x) = \frac{\mu}{\beta}\frac{\mathrm{d}}{\mathrm{d}x}n(x) + \mu n(x)\frac{\mathrm{d}}{\mathrm{d}x}E_{\mathrm{c}}(x) \tag{27}$$

which determines $n(x)$ in terms of $E_{\mathrm{c}}(x)$ and the constant parameter j. On the other hand, when the current is ballistic in an interval (x_{i-1}^N, x_i^N) [cf. equation (4)], only the equilibrium densities $n(x_{i-1}^N), n(x_i^N)$ at the end points of the interval enter into the description, and an averaging formalism must be provided which allows one to derive from these discrete values of the density a continuous physical density to be used in the Poisson equation.

We close this section with a brief discussion of the special case of a single barrier. In the case of a single grain boundary or a Schottky contact, the band edge profile exhibits a single peak and no valleys, so that the shape term vanishes, $\widetilde{\Lambda} = 0$, and equations (22) and (23) yield

$$j = -ev_{\mathrm{e}}N_{\mathrm{c}}\,\mathrm{e}^{-\beta E_p}\frac{l}{l + \widetilde{S}}\left(1 - \mathrm{e}^{-\beta eV}\right). \tag{28}$$

For a grain boundary, the barrier height E_{p} is given by the difference of the profile maximum at the boundary and the Fermi level in the bulk of the grain. The barrier height of a Schottky contact is equal to the difference of the profile maximum in the semiconductor and the Fermi level of the metal. Equation (28) is equivalent to equation (6) of [5]. However, the present derivation is different from that of [5], the averaging over ballistic configurations being the crucial ingredient.

If the mean free path is much longer than the reduced sample length, $l \gg \widetilde{S}$, one obtains from equation (28) the thermionic-emission formula [1, 2]. In the opposite case, $l \ll \widetilde{S}$, the transport mechanism is diffusive; with the use of

$$\mu = ev_{\mathrm{e}}\beta l \tag{29}$$

equation (28) becomes

$$j = -\frac{\mu N_{\mathrm{c}}\mathrm{e}^{-\beta E_p}}{\beta\widetilde{S}}\left(1 - \mathrm{e}^{-\beta eV}\right). \tag{30}$$

Looking at the diffusive limit differentially, we have from equation (4) in conjunction with equation (25), replacing the discrete coordinate x_i^N with the continuous coordinate x, i.e. setting $x_i^N = il = x$ $(i = 1, \ldots, N)$, $l = S/N$ with $N \to \infty$,

$$j = \beta e v_e N_c e^{-\beta[E_c(x)-E_F(x)]}[dE_F(x)/dx] \cdot l = \mu n(x) \frac{d}{dx} E_F(x) \tag{31}$$

in agreement with equation (27).

3.2. Quantum effects

Since we are focusing attention on the case where the mean free path and the relevant structures of the band edge profile are of comparable length, we are generally dealing with systems of small dimensions and therefore must expect quantum effects such as discretization of energy states and tunnelling to play a role. Considering, e.g. a potential valley with a width of the order of 20 nm, as typified by the examples discussed below, we find that the electron motion is quantized with energy spacings of about 0.03 eV. Since the barrier heights in the examples exceed this value by an order of magnitude, one may still speak of a classical continuum of states. On the other hand, the wave length of the electrons at $T = 300$ K is $\lambda = h/(m^* v_e) \approx 10$ nm, so that quantum tunnelling should be important. The formalism for including the effect of tunnelling, i.e. for going from thermionic emission to thermionic field emission, will be developed in the following. We do not include the effects of phase interference and localization, since these are not expected to play an important role for the polycrystalline materials we are considering.

The transmission probabilities for ballistic intervals with no peaks inside are treated classically, as before. Tunnelling has to be taken into account near each peak in intervals $X_n^- < x < X_n^+$ containing the peak at X_n $(n = 0, 1, \ldots, M)$. Since we can treat only *ballistic* quantum transport, these intervals must not contain equilibration points. In other words, in these intervals we must effectively set $l \to \infty$, and in the integrals over x these intervals are omitted, since here $dx/l = 0$. The lengths to be chosen for the intervals $[X_n^-, X_n^+]$ will be discussed below.

In WKB approximation, the thermally averaged quantal probability $\mathcal{T}^{WKB}(i)$ for ballistic transmission from x_{i-1}^N to x_i^N is given by

$$\mathcal{T}^{WKB}(i) = e^{-\beta E_c^m(i)} + \beta \int_{E_c^{(i)}}^{E_c^m(i)} dE \; \exp\left(-\beta E - \frac{2}{\hbar} \int_{y_i}^{y_i^*} dx \{2m^*[E_c(x) - E]\}^{1/2}\right) \tag{32}$$

where $E_c^{(i)}$ is defined after equation (3). The limits of integration y_i and y_i^* are the turning points at energy E on either side of the peak (if the interval $\{i\} = [x_{i-1}^N, x_i^N]$ contains several peaks, the integral in the exponential goes from the left-most turning point to the right-most).

It is found that in the current-voltage characteristic (23), the barrier factor $\exp(-\beta E_p)$ is to be multiplied by the tunnelling correction $\mathcal{C}^{-1}$, with

$$\mathcal{C} = e^{-\beta[E_c^m - E_c(X_0^-)]} \times \left[e^{-(X_M^- - X_0^+)/l} \left(\frac{1}{\mathcal{T}^{WKB}(X_0^-, X_M^+)} - \frac{1}{\mathcal{T}^{WKB}(X_0^-, X_0^+)} \right) + \frac{1}{\mathcal{T}^{WKB}(X_0^-, X_0^+)} \right] \tag{33}$$

where the notation $\mathcal{T}^{WKB}(X_0^-, X_M^+)$ refers to the averaged WKB transmission probability $\mathcal{T}^{WKB}(i)$ for the interval $[X_0^-, X_M^+]$, etc; here, X_0 is the position of the overall maximum peak E_c^m. The reduced sample length $\widetilde{S}$ and the shape term $\widetilde{\Lambda}$ that enter the effective transport length L [cf. equation (22)] now appear as

$$\widetilde{S} = \mathcal{C}^{-1} \int_0^{S^\bullet} dx \, e^{-\beta[E_c^m - E_c(x)]} \tag{34}$$

where the upper limit $S^{\bullet}$ implies that all intervals $[X_n^-, X_n^+]$ ($n = 0, 1, \ldots, M$) are to be omitted, and

$$\widetilde{\Lambda} = \mathcal{C}^{-1} \sum_{v=1}^{M} \int_{X_v^{-\bullet}}^{X_v^-} \mathrm{d}x \, \mathrm{e}^{-|x-x^*|/l} \, \mathrm{e}^{-\beta E_\mathrm{c}^\mathrm{m}} \left[A_v \, \mathrm{e}^{\beta E_\mathrm{c}(X_v)} - \mathrm{e}^{\beta E_\mathrm{c}(x)} \right] \tag{35}$$

with $X_v^{-\bullet} = \max\{X_v^{-*}, X_{v-1}^+\}$ and

$$A_v = \mathcal{T}\left(X_v^-, X_v^+\right) / \mathcal{T}^{\mathrm{WKB}}\left(X_v^-, X_v^+\right) \qquad v = 1, \ldots, M \tag{36}$$

where $\mathcal{T}$ is the average classical transmission probability (3). It can be shown that $\widetilde{\Lambda} < S$, as in the classical case.

For a single barrier, equation (28) is generalized to

$$j = -ev_\mathrm{e} N_\mathrm{c} \, \mathcal{C}^{-1} \, \mathrm{e}^{-\beta E_p} \frac{l}{l + \widetilde{S}} \left(1 - \mathrm{e}^{-\beta eV}\right). \tag{37}$$

According to equation (34), $\widetilde{S}$ includes the tunnelling correction factor $\mathcal{C}^{-1} \geqslant 1$, and thus tunnelling enhances the relative effect of the non-ballistic part of the electron motion embodied in the term $\widetilde{S}$ in the denominator of expression (37).

The intervals $[X_n^-, X_n^+]$ enclosing the peaks at X_n are defined as the intervals in which tunnelling plays a role; they are determined by the requirement that the ratio A_v becomes virtually independent of the length of the interval if that extends beyond the end points $X_n^{\pm}$. On the other hand, it must be ascertained that these lengths are smaller than the mean free path l, otherwise the quantum correction scheme breaks down: if tunnelling takes place over distances larger than the mean free path, thermalization and tunnelling occur simultaneously, which cannot be described in the present framework. Explicit calculations of the quantum corrections will be carried out below.

3.3. The degenerate case

In the degenerate case, a simple treatment is possible only in the limit of zero bias. Formula (2) for the current is to be replaced (for infinitesimal bias) with

$$j(i) = \frac{4\pi em^*}{\beta h^3} \, \delta_i \, \frac{\partial}{\partial E_\mathrm{F}} \int_{E_\mathrm{c}^{(i)}}^{\infty} \mathrm{d}E \; T_i(E) \; \ln\left(1 + \mathrm{e}^{-\beta[E - E_\mathrm{F}]}\right) \tag{38}$$

where we have set $E_\mathrm{F}(x_{i-1}^N) = E_\mathrm{F}$ and $E_\mathrm{F}(x_i^N) = E_\mathrm{F} + \delta_i$. Classically, this becomes

$$j(i) = \frac{4\pi em^*}{\beta h^3} \delta_i \; \ln\left(1 + \mathrm{e}^{-\beta[E_\mathrm{c}^\mathrm{m}(i) - E_\mathrm{F}]}\right) \; . \tag{39}$$

By analogy with equation (6), we then find

$$E_\mathrm{F}(S) - E_\mathrm{F}(0) = \sum_{i=1}^{N} \delta_i = j \, \frac{\beta h^3}{4\pi em^*} \sum_{i=1}^{N} \frac{1}{\ln\left(1 + \mathrm{e}^{\beta[E_\mathrm{F} - E_\mathrm{c}^\mathrm{m}(i)]}\right)} \tag{40}$$

with $E_\mathrm{F}(0)$ and $E_\mathrm{F}(S)$ differing infinitesimally from the equilibrium value E_F. Denoting here the average over the sum (cf. section 2.1), multiplied by $\ln(1 + \mathrm{e}^{\beta[E_\mathrm{F} - E_\mathrm{c}^\mathrm{m}]})$, by Ξ_d,

$$\Xi_\mathrm{d} = \left\langle \sum_{i=1}^{N} \frac{\ln\left(1 + \mathrm{e}^{\beta[E_\mathrm{F} - E_\mathrm{c}^\mathrm{m}]}\right)}{\ln\left(1 + \mathrm{e}^{\beta[E_\mathrm{F} - E_\mathrm{c}^\mathrm{m}(i)]}\right)} \right\rangle_{\{N, x_i^N\}} \tag{41}$$

we have

$$eV = E_\mathrm{F}(S) - E_\mathrm{F}(0) = -j \, \frac{\beta h^3}{4\pi em^*} \, \frac{1}{\ln\left(1 + \mathrm{e}^{\beta[E_\mathrm{F} - E_\mathrm{c}^\mathrm{m}]}\right)} \, \Xi_\mathrm{d}. \tag{42}$$

The calculation of the average sum Ξ_d follows section 2.2. A (classical) effective transport length L_d is introduced as

$$L_d = \Xi_d\, l = l + \widetilde{S}_d + \widetilde{\Lambda}_d \tag{43}$$

where

$$\widetilde{S}_d = \int_0^S dx\, \frac{\ln\left(1 + e^{\beta[E_F - E_c^m]}\right)}{\ln\left(1 + e^{\beta[E_F - E_c(x)]}\right)} \tag{44}$$

is the reduced sample length for the degenerate case, in generalization of equation (15), and

$$\widetilde{\Lambda}_d = \sum_{v=1}^{M} \int_{X_v^*}^{X_v} dx\, e^{-|x - x_v^*|/l} \left[\frac{\ln\left(1 + e^{\beta[E_F - E_c^m]}\right)}{\ln\left(1 + e^{\beta[E_F - E_c(X_v)]}\right)} - \frac{\ln\left(1 + e^{\beta[E_F - E_c^m]}\right)}{\ln\left(1 + e^{\beta[E_F - E_c(x)]}\right)} \right] \tag{45}$$

is the generalization of the shape term (21). The zero-bias conductance per unit area, finally, is obtained as

$$g = \left(\frac{|j|}{V}\right)_{V \to 0} = \frac{4\pi e^2 m^*}{\beta h^3}\, \ln\left(1 + e^{-\beta E_p}\right)\, \frac{l}{L_d} \tag{46}$$

with $E_p = E_c^m - E_F$ (note that in the degenerate case, E_p may be negative). Quantum effects may be taken into account as in the nondegenerate case.

3.4. The effect of dimensionality

The samples we consider are assumed to have a parallel-plane structure and thus have an essentially one-dimensional geometry. Nevertheless, the treatment of the transport process itself should, of course, be three-dimensional. Therefore, in the discussion preceding equation (9), one must consider the distance between collisions, ξ, in three-dimensional space. This introduces a polar angle to be summed over appropriately in averaging over the ballistic configurations, thereby rendering the formalism appreciably more complicated. In our effort to obtain a simple, *closed* formula for the current-voltage characteristic, we have restricted ourselves to a one-dimensional formulation, which leads to the desired result in a straightforward way.

Now, for the special case of a *constant* profile, $E_c(x) = 0$, de Jong [29] has derived a formula which describes the transition from the (ballistic) Sharvin resistance [30] to the (diffusive) Drude zero-bias conductance [15,31]. In this work, use is made of an integro-differential equation in two and three dimensions, leading to a result which, for the three-dimensional case, is summarized in the formula [in the notation of our equation (46) with $E_c^m = 0$ and $\beta E_F \gg 1$]

$$g = \frac{4\pi e^2 m^* E_F}{h^3}\, \frac{l}{l + \frac{3}{4}\gamma S} \tag{47}$$

where the (numerically determined) factor γ increases monotonically from 1 to 4/3 as l/S goes from 0 (diffusive limit) to ∞ (ballistic limit). In our one-dimensional formulation, the denominator in formula (47) reads simply $l + S$. We therefore suggest that the restriction to a one-dimensional formulation introduces a numerical error of perhaps 30%; the main features of our model, which the following examples show to involve enhancements by factors of 10, should not be severely affected.

Unfortunately, one cannot make use of differential equations in the more general case when the profile $E_c(x)$ changes significantly over distances of the order of the mean free path l. Anyhow, we are not so much interested in the numerical solution of the transport problem (which would most efficiently be handled by Monte Carlo simulations) but, as far as possible, in its physical analysis via simple and transparent closed formulas.

4. Examples

4.1. Zero-bias conductivity of a chain of identical grains

The zero-bias conductance per unit area, $g = (|j|/V)_{V\to 0}$, is obtained as

$$g = \beta e^2 v_e N_c \mathcal{C}^{-1} e^{-\beta E_p} \frac{l}{L} = \frac{4\pi e^2 m^*}{\beta h^3} \mathcal{C}^{-1} e^{-\beta E_p} \frac{l}{L}. \tag{48}$$

The band edge profile $E_c(x)$ for zero bias is given by its equilibrium shape, and is calculated as a solution of the Poisson equation (24) in the trapping model.

We consider a chain of ν identical grains, each of length s, as shown in figure 3. There are $\nu - 1$ identical valleys in $E_c(x)$. Writing $\widetilde{S} = \nu\widetilde{s}$ and $\widetilde{\Lambda} = (\nu-1)\widetilde{l}$, we have from equation (22)

$$L = l + \nu\widetilde{s} + (\nu - 1)\widetilde{l}. \tag{49}$$

As mentioned above, the profile $E_c(x)$, and therefore also the barrier height E_p, the reduced grain length $\widetilde{s}$, and the single-grain shape term $\widetilde{l}$, indirectly depend on the mean free path l via its connection with the donor density N_{don}. The l-dependence of the main feature of the profile, the barrier height E_p, can be read from the l-dependence of the conductance g for a single grain in the ballistic regime, when $L = l$ in equation (48).

The term l in expression (49) for the effective transport length L represents the ballistic contribution to the current. For purely ballistic motion ($l \gg \nu s$ and $L \to l$), one finds from equation (48) in the classical limit ($\mathcal{C} = 1$) that only *one* barrier, the front barrier, is relevant since it eclipses all others (cf. above, and also the discussion in section 2 of [32]). However, when tunnelling takes place (possibly through several neighbouring peaks), equation (37) in conjunction with equation (33) is to be used to obtain the conductance.

For the purpose of illustration, we consider two silicon samples with grain length $s = 30$ nm (μc-Si) and $s = 100$ nm (pc-Si), respectively. Instead of the zero-bias conductance g, we introduce here the zero-bias conductivity σ as conductance times sample length,

$$\sigma = gS = g\nu s \tag{50}$$

(in the diffusive limit, σ is independent of the number of grains ν). The conductivity has been calculated at temperature $T = 300$ K by means of formulas (48) and (49) as a function of the donor density N_{don}. Applying the criteria discussed in the final paragraph of section 3.2, the length of the 'tunnelling intervals' $[X_n^-, X_n^+]$ enclosing the peaks was taken to be 6 nm (which, not surprisingly, is of the order of the wave length $\lambda = 10$ nm of the electrons); this value is much smaller than the magnitude of the mean free path in all cases considered. The results are shown in figure 4 as a function of the *mean free path* l, employing the connection between l

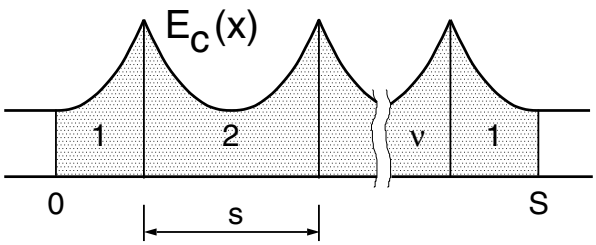

Figure 3. Equilibrium band edge profile $E_c(x)$ of a chain of ν identical grains of length s, forming a sample of total length $S = \nu s$.

and N_{don} obtained from [28] and displayed in the inset. It is seen that the conductivity depends appreciably on the number of grains in the case of the smaller grain size, $s = 30$ nm. Thus it emerges that the conductivity calculated for a single grain cannot simply be carried over to the entire microcrystalline sample. The latter must be considered as a whole; there is in this case no grain-specific conductivity.

Tunnelling has a direct influence on the barrier transmission probability, which is taken into account through the correction factor $\mathcal{C}^{-1}$ in equation (48). It enhances the transmission probability by up to 50% in the region of small l.

In figure 5, we summarize the results of the unified model in comparison to those of the drift-diffusion and thermionic-emission models. Since tunnelling does not affect appreciably the mutual relation between the different transport models, we here consider only the *classical* conductivities, and plot these *relative to the conductivity within the drift-diffusion model,* σ_{DD} [with $L = \nu\tilde{s}$ in equation (48)]. The curves labelled UM(1) and UM(100) represent the conductivity of the unified model for a chain of one and a hundred grains, respectively, divided by the conductivity calculated within the drift-diffusion model. In the regions where

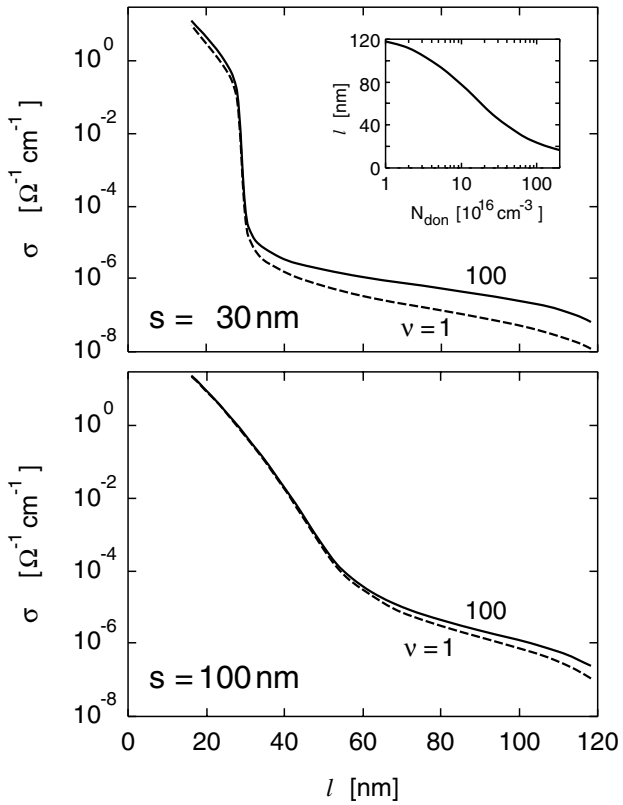

Figure 4. Zero-bias conductivity σ in the unified model for Si samples with grain length $s = 30$ nm (upper panel) and grain length $s = 100$ nm (lower panel), plotted as a function of mean free path l for temperature $T = 300$ K, trapping state density $N_{\mathrm{t}} = 2 \times 10^{12}$ cm^{-2}, and a single trapping level located at 0.56 eV above the valence band edge. Dashed curves: single grain ($\nu = 1$); solid curves: chain of a hundred grains ($\nu = 100$). The inset in the upper panel shows the relation between l and the donor density N_{don} at $T = 300$ K.

these curves approach unity, the transport mechanism is predominantly diffusive. The curve labelled TE ('thermionic emission') represents the relative conductivity for purely ballistic transport across a *single* grain boundary, the result being identified (as is usually done) with the conductivity of the entire chain. This procedure ignores the eclipsing effect alluded to above, and is justified only if the mean free path is long compared to the width of the barrier but short compared to the length of the grain [cf. the conditions leading to equation (19)], so that while moving through the grain, the electrons are thermalized and 'face' each grain boundary barrier with the same thermal distribution as when passing over the previous one.

We see that the transport mechanism tends to become diffusive for very small values of l, and also for $l > 80$ nm in the case $\nu = 100$; this holds for $s = 30$ nm as well as for $s = 100$ nm. The thermionic-emission model yields acceptable results in the region $20 < l < 60$ nm at $s = 100$ nm for $\nu = 1$ and $\nu = 100$. At $s = 30$ nm, it is valid for $\nu = 1$ but completely invalid for $\nu = 100$. In the latter case, neither the drift-diffusion nor the thermionic emission models describe adequately the correct mechanism [which is represented by the curve labelled UM(100)].

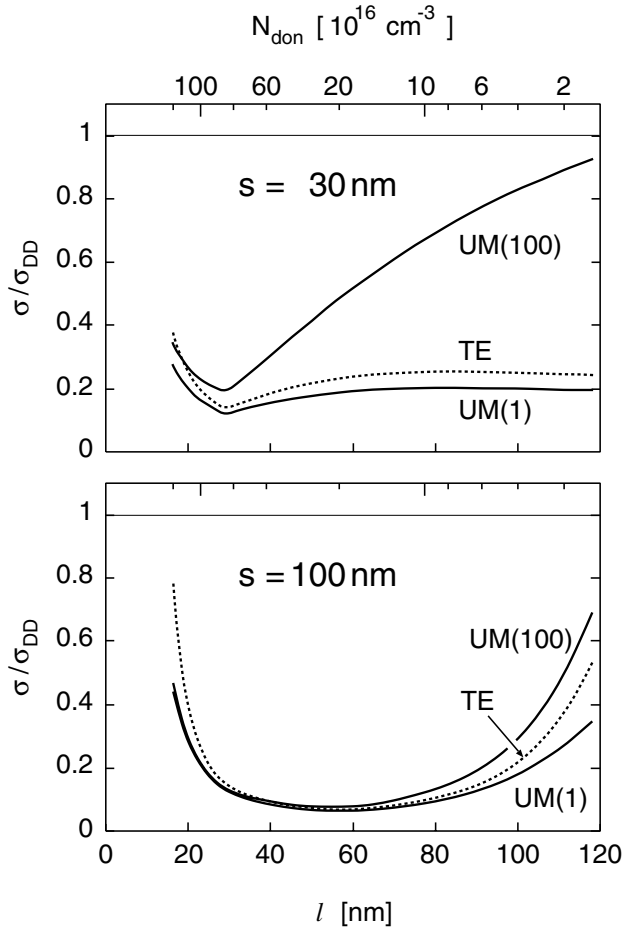

Figure 5. Relative conductivities $\sigma/\sigma_{\mathrm{DD}}$ for the cases of figure 4.

The transport properties have been discussed here for just two grain lengths s representative of microcrystalline and polycrystalline silicon, respectively. A more comprehensive study would have to deal with the s-dependence over a suitably broad range, which in particular may lead to the disclosure of possible scaling properties.

4.2. Degenerate case: single barrier

We apply formula (46) to transport through a single grain boundary. Choosing parameter values so as to reproduce approximately the conditions of the example of [11], we consider the temperature dependence of the conductance for a grain boundary barrier in highly doped pc-SnO_2:Sb with grain length $s = 50$ nm. We have calculated the equilibrium band edge profile $E_c(x)$ at $T = 300$ K and $N_{don} = 7.2 \times 10^{18}$ cm^{-3}, corresponding to a mean free path $l = 11$ nm. We assume a single trapping level at midgap (1.75 eV above the valance band edge) with trapping state density $N_t = 1.95 \times 10^{12}$ cm^{-2}. The barrier height is obtained as $E_p = 0.038$ eV and the barrier width as ≈ 6 nm. Since we intend to apply formula (46) in a schematic manner only and the band edge profile is found to depend only weakly on T and N_{don} (or E_F), we adopt the profile calculated at $T = 300$ K for all values of T and control the degree of degeneracy by independently choosing the value of E_F in equation (46).

In figure 6, we display the T-dependence of the barrier conductivity $\sigma = gS$, calculated from equation (46) using for the mean free path the fixed value $l = 11$ nm (when comparing with the results of [11], one must take account of the factor $\alpha_{eff} \approx 10^{-2}$ introduced there). The case considered here [$E_F = 3.52$ eV, compared to E_c(grain bulk) = 3.50 eV] is strongly degenerate; nevertheless, the results of calculations using Boltzmann and Fermi–Dirac statistics [UM(non-d) vs. UM(d)] are not too far apart. Further, it is observed, by comparing the curves labelled UM(d) and UM(d,cl), that the effect of tunnelling increases the conductivity by more than a factor of two, becoming stronger as the temperature decreases.

The purely diffusive and ballistic (degenerate) conductivities are also shown in figure 6. It appears that, as the temperature rises, the transport character in the unified model changes from ballistic to diffusive. This is governed by the relative size of the terms l and $\widetilde{S}_d$ in the effective transport length L_d appearing in the denominator of expression (46) for the conductance g.

Formula (44) yields for $\widetilde{S}_d$ a value which increases with E_F, i.e. with donor density N_{don}. In [11], the corresponding term $\frac{3}{4}w$ is found (by fitting to data) to decrease instead; a more detailed analysis appears to be necessary for an explanation of this discrepancy.

5. Summary and conclusions

For electron transport in parallel-plane semiconducting structures, we have developed a generalized Drude model which unifies ballistic and diffusive transport for arbitrary magnitude of the mean free path and arbitrary shape of the conduction band edge profile. The semiclassical approach has been adopted, but tunnelling has been taken into account in WKB approximation.

The basic assumption of the model is that the electrons move ballistically over intervals whose lengths are randomly distributed about the value of the mean free path. By averaging over the random configurations of ballistic intervals, we have derived simple formulas for the current-voltage characteristic (in the nondegenerate case) and for the zero-bias conductance (in the degenerate case). The distinctive feature of these formulas is the presence of an effective length that comprises a shape term directly manifesting the interplay of ballistic and diffusive transport. Previously obtained formulas for the current-voltage characteristic and for the zero-bias conductance refer to special cases and do not include such a term.

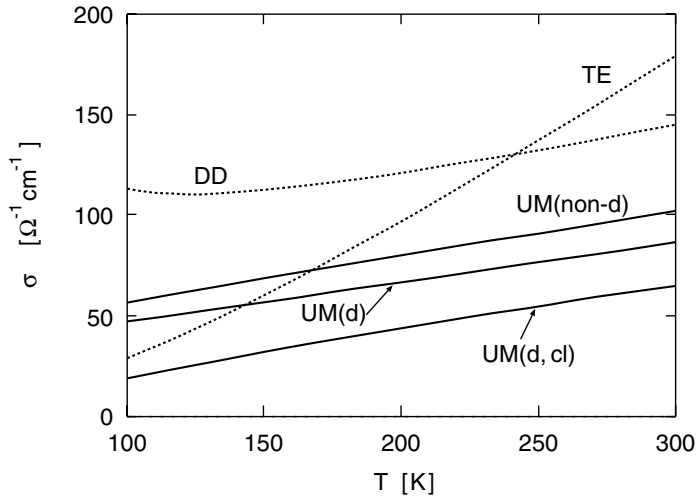

Figure 6. Temperature dependence of the barrier conductivity σ for a grain boundary barrier in pc-SnO_2:Sb with conduction band edge profile calculated for the fixed parameter values $s = 50$ nm, $T = 300$ K, $N_{\rm don} = 7.2 \times 10^{18}$ cm^{-3} ($l = 11$ nm), $N_{\rm t} = 1.95 \times 10^{12}$ cm^{-2}, and a single-trapping level located at 1.75 eV above the valence band edge. The Fermi level is chosen as $E_{\rm F} = 3.52$ eV. UM(d): unified model for the degenerate case (Fermi-Dirac statistics); UM(non-d): unified model for the nondegenerate case (Boltzmann statistics); DD: drift-diffusion model; TE: ballistic model; UM(d, cl): unified model for the degenerate classical case (no tunnelling).

We have performed numerical calculations of the zero-bias conductivity for chains of grains of (nondegenerate) μc-Si and pc-Si, and for a single grain boundary in highly doped (degenerate) pc-SnO_2:Sb. The calculations for Si show substantial deviations of the results of the unified model from those of the purely ballistic and purely diffusive models. Moreover, within the unified model, one finds a fairly strong dependence of the conductivity on the number of grains.

For the calculation of the zero-bias conductivity, the band edge profile to be used is the equilibrium profile. Except in this case and in the diffusive limit, the determination of the band edge profile is highly complicated in general. Basically, one has to solve the Poisson equation along with the relevant current equation self-consistently, taking into account the averaging of the electron density over configurations of ballistic intervals.

In this work, we have considered transport in one dimension; it has been argued that this should be sufficient to exhibit the essential features of the physical phenomena involved. Possible generalizations would be the inclusion of the coupling to minority carriers, of optically induced carrier generation and of recombination.

References

[1] Bethe H A 1942 *MIT Radiat Lab Rep* **43–12**
[2] Sze S M 1981 *Physics of Semiconductor Devices* (New York: Wiley)
[3] Schottky W 1938 *Naturwissenschaften* **26** 843
[4] Mott N F 1938 *Proc. Cambridge Philos. Soc.* **34** 568
[5] Crowell C R and Sze S M 1966 *Solid-State Electron.* **9** 1035
[6] McGonigal G C, Thomson D J, Shaw J G and Card H C 1983 *Phys. Rev.* B **28** 5908
[7] Simeonov S S 1987 *Phys. Rev.* B **36** 9171

[8] Evans P V and Nelson S F 1991 *J. Appl. Phys.* **69** 3605
[9] McKelvey J P, Longini R L and Brody T P 1961 *Phys. Rev.* **123** 51
[10] Lu N C C, Gerzberg L, Lu C Y and Meindl J D 1981 *IEEE Electron Dev. Lett.* **EDL-2** 95
[11] Prins M W J, Grosse-Holz K-O, Cillessen J F M and Feiner L F 1998 *J. Appl. Phys.* **83** 888
[12] Ashcroft N W and Mermin N D 1976 *Solid State Physics* (Fort Worth: Harcourt Brace)
[13] Dolan W W and Dyke W P 1954 *Phys. Rev.* **95** 327
[14] Stratton R 1962 *Phys. Rev.* **125** 67
[15] Drude P 1900 *Ann. Physik* **1** 566
Drude P 1900 **3** 369
[16] Sapoval B and Hermann C 1995 *Physics of Semiconductors* (Berlin: Springer)
[17] Baranger H U and Stone A D 1989 *Phys. Rev.* B **40** 8169
[18] Imry Y and Landauer R 1999 *Rev. Mod. Phys.* **71** S306
[19] Landauer R 1987 *Z. Phys.* B **68** 217
[20] Landauer R 1989 *J Phys.: Condens. Matter* **1** 8099
[21] Stone A D and Szafer A 1988 *IBM J. Res. Develop.* **32** 384
[22] Duke C B 1969 *Tunneling in Solids*, in *Solid State Phys. Suppl.* Vol. 10 ed F Seitz, D Turnbull and H Ehrenreich (New York: Academic Press)
[23] Yang K, East J R and Haddad G I 1993 *Solid-State Electron.* **36** 321
[24] Kamins T I 1971 *J. Appl. Phys.* **42** 4357
[25] Seto J Y W 1975 *J. Appl. Phys.* **46** 5247
[26] Weis T, Lipperheide R and Wille U 1998 *Proc. 2nd World Conf. Exhib. Photovoltaic Solar Energy Conversion, Vienna* ed J Schmid, H A Ossenbrink, P Helm, H Ehmann and E D Dunlop (European Comm. Joint Res. Centre, Ispra) p 1438
[27] Weis T 1999 *PhD Thesis* Free University Berlin
[28] Arora N D, Hauser J R and Roulston D J 1982 *IEEE Trans. Electron Devices* **ED-29** 292
[29] de Jong M J M 1994 *Phys. Rev.* B **49** 7778
[30] Sharvin Yu V 1965 *Zh. Eksp. Teor. Fiz.* **48** 984
Sharvin Yu V 1965 *Sov. Phys. JETP* **21** 655
[31] Maxwell J C 1891 *A Treatise on Electricity and Magnetism* (New York: Dover Press)
[32] Kim D M, Khonder A N, Ahmed S S and Shah R R 1984 *IEEE Trans. Electron Devices* **ED-31** 480